Gaussian quadrature and lattice discretization of the Fermi-Dirac distribution for graphene

D. Oettinger,[1] M. Mendoza,[2,*] and H. J. Herrmann[2,3]
[1]*ETH Zürich, Department of Physics, CH-8093 Zürich, Switzerland*
[2]*ETH Zürich, Computational Physics for Engineering Materials, Institute for Building Materials, Schafmattstrasse 6, HIF, CH-8093 Zürich, Switzerland*
[3]*Departamento de Física, Universidade Federal do Ceará, Campus do Pici, 60455-760 Fortaleza, Ceará, Brazil*
(Received 2 May 2013; published 3 July 2013)

We construct a lattice kinetic scheme to study electronic flow in graphene. For this purpose, we first derive a basis of orthogonal polynomials, using as the weight function the ultrarelativistic Fermi-Dirac distribution at rest. Later, we use these polynomials to expand the respective distribution in a moving frame, for both cases, undoped and doped graphene. In order to discretize the Boltzmann equation and make feasible the numerical implementation, we reduce the number of discrete points in momentum space to 18 by applying a Gaussian quadrature, finding that the family of representative wave $(2+1)$-vectors, which satisfies the quadrature, reconstructs a honeycomb lattice. The procedure and discrete model are validated by solving the Riemann problem, finding excellent agreement with other numerical models. In addition, we have extended the Riemann problem to the case of different dopings, finding that by increasing the chemical potential the electronic fluid behaves as if it increases its effective viscosity.

DOI: 10.1103/PhysRevE.88.013302 PACS number(s): 02.70.−c, 72.80.Vp, 73.63.−b, 05.30.−d

I. INTRODUCTION

Since its discovery [1,2], graphene has shown a series of wonderful electrical and mechanical properties, such as ultrahigh electrical conductivity, ultralow viscosity, and exceptional structural strength, combined with mechanical flexibility and optical transparence. Due to the special symmetries of the honeycomb lattice, electrons in graphene are shown to behave like *massless* chiral ultrarelativistic quasiparticles, propagating at a Fermi speed of about $v_F \sim 10^6$ m/s [3,4]. This places graphene as an appropriate laboratory for experiments involving relativistic massless particles confined to a two-dimensional space [5].

Electronic gas in graphene can be approached from a hydrodynamic perspective [6–9], in the regime of low doping (i.e., Fermi energy lower than thermal energy), high temperatures (where the carriers are mostly due to thermal excitations), and low drift velocities. Under such conditions, electrons in graphene behave as a nearly perfect fluid reaching viscosities significantly smaller than those of superfluid helium at the λ point. This has suggested the possibility of observing preturbulent regimes, as explicitly pointed out in Ref. [6] and later confirmed by numerical simulations [10]. All these characteristics in graphene open up the possibility of studying several phenomena known from classical fluid dynamics, e.g., transport through disordered media [11] and Kelvin-Helmholtz and Rayleigh Bénard instabilities, just to name a few. However, the study of these phenomena needs appropriate numerical tools, which take into account both the relativistic effects and the Fermi-Dirac statistics.

Recently, a solver for relativistic fluid dynamics based on a minimal form of the relativistic Boltzmann equation, whose dynamics takes place in a fully discrete phase-space lattice and time, known as relativistic lattice Boltzmann (RLB), has been proposed by Mendoza *et al.* [12,13] (and subsequently revised in Ref. [14] enhancing numerical stability). This model reproduces correctly shock waves in quark-gluon plasmas, showing excellent agreement with the solution of the full Boltzmann equation obtained by Xu and Greiner [15] and Bouras *et al.* [16] using BAMPS (Boltzmann approach multiparton scattering). In order to set up a theoretical background for the lattice version of the relativistic Boltzmann equation for the Boltzmann statistics, Romatschke *et al.* [17] developed a scheme for an ultrarelativistic gas based on the expansion in orthogonal polynomials of the Maxwell-Jüttner distribution [18] and, by following a Gauss-type quadrature procedure, the discrete versions of the distribution and the weight functions were calculated. This procedure was similar to the one used for the nonrelativistic lattice Boltzmann model [19–25]. This relativistic model showed very good agreement with theoretical data, although it was not compatible with a lattice, thereby requiring linear interpolation in the free-streaming step. Another model based on a quadrature procedure was developed recently in order to make the relativistic lattice Boltzmann model compatible with a lattice [26]. However, all these models are based on the the Maxwell-Jüttner distribution, which is based on the Boltzmann statistics, and therefore their applications to quantum systems is limited.

In this work, we construct a family of orthogonal polynomials by using the Gram-Schmidt procedure using as the weight function the ultrarelativistic Fermi-Dirac distribution at rest. By applying a Gauss-type quadrature, we find that the family of discrete $(2+1)$-momentum vectors needed to recover the first three moments of the equilibrium distribution are fully compatible with a hexagonal lattice, avoiding any type of linear interpolation. This result is very convenient, since the crystal of graphene shares the same geometry, facilitating the implementation of boundary conditions, allowing for instance having a good approximation for the electronic transport in nanoribbons with armchair or zigzag edges [27,28] by implementing the typical bounce-back rule for lattice Boltzmann models.

*mmendoza@ethz.ch

The paper is organized as follows: in Sec. II, we describe in detail the expansion of the Fermi-Dirac distribution in an orthogonal basis of polynomials and perform the Gauss-type quadrature. In this section, we also explain the discretization procedure. In Sec. III, we implement the validation of our model by simulating the Riemann problem, and in Sec. IV, we perform additional simulations for doped graphene. Finally, in Sec. V, we discuss the results and future work.

II. MODEL DESCRIPTION

The electronic gas in graphene can be considered as a gas of massless Dirac quasiparticles obeying the Fermi-Dirac statistics in a two-dimensional space. Thus, we define the single-particle distribution function $f(x^\mu,p^\mu)$ in phase space, with $x^\mu=(x^0,x^1,x^2)$ and $p^\mu=(p^0,p^1,p^2)$ being the time-position and energy-momentum coordinates, respectively. Here x^0 denotes time, $\vec{x}=(x^1,x^2)$ the spatial coordinates, p^0 the energy, and $\vec{p}=(p^1,p^2)$ the momenta of the particles. In the ultrarelativistic regime, we get $p^\mu p_\mu=0$ (in this paper we use the Einstein notation; i.e., repeated indexes denote summing over such indexes). In our approach, we assume that the distribution function f evolves according to the relativistic Boltzmann-Bhatnagar-Gross-Krook (BGK) equation [18],

$$p^\mu\partial_\mu f=-\frac{p_\alpha U^\alpha}{v_F^2\tau}(f-f_{\rm eq}), \tag{1}$$

where τ is the relaxation time and $f_{\rm eq}$ the equilibrium distribution, which in our case, is the relativistic Fermi-Dirac distribution defined by

$$f_{\rm eq}(x^\mu,p^\mu)=\frac{1}{e^{(p_\alpha U^\alpha-\mu)/k_BT}+1}, \tag{2}$$

with T being the temperature, k_B the Boltzmann constant, U^μ the macroscopic $(2+1)$-velocity of the fluid [18,29,30], and μ the chemical potential. The relation between the Lorentz-invariant U^μ and the classical velocity $\vec{u}=(u^1,u^2)$ is given by $U^\mu=\gamma(v_F,u^1,u^2)$, with v_F being the Fermi speed and $\gamma=1/\sqrt{1-\vec{u}^2/v_F^2}$.

A. Moment expansion

Here, we perform an expansion of the Fermi-Dirac distribution, Eq. (2), in an orthogonal basis of polynomials. In our case, since we are interested in the hydrodynamic regime, we truncate the expansion preserving only the polynomials up to second order, although achieving higher orders is also possible by using the same procedure. In particular, we need to reproduce the first three moments of the equilibrium Fermi-Dirac distribution, namely, $\langle 1\rangle_{\rm (eq)}$, $\langle p^\alpha\rangle_{\rm (eq)}$, and $\langle p^\alpha p^\beta\rangle_{\rm (eq)}$, for $\alpha,\beta=0,1,2$. The angular brackets denote expectation values using the distribution f via $\langle Q\rangle=\int d\mu\, Qf$, with $d\mu=d^2p/2p^0(2\pi)^2$, and the subscript $_{\rm (eq)}$ indicates that the equilibrium distribution $f_{\rm eq}$ is taken instead of f.

This method was originally introduced by Grad [31] who expanded the Maxwell-Boltzmann distribution in Hermite polynomials, based on the fact that they are orthogonal, using as the weight function the Maxwellian distribution at rest. In this spirit, we derive a new basis of polynomials that are orthogonal with respect to the Fermi-Dirac distribution at rest,

$$w(p_0)=\frac{1}{e^{p_0/k_BT}+1}. \tag{3}$$

Note that for the nonrelativistic case, the Maxwell-Boltzmann distribution corresponds to the generating function of the Hermite polynomials. However, this is not the case in relativity with the Fermi-Dirac distribution, since due to the Lorentz transformation and the Fermi-Dirac statistics the weight function $w(p_0)$ evaluated at a moving frame leads to a non- relation, $w(p_\mu U^\mu)$, which cannot be written easily in the form of a known generating function. Indeed, the Maxwell-Jüttner distribution can be written as the generating function of the Laguerre polynomials, but for the Fermi-Dirac statistics this does not apply.

For the following derivations it is useful to choose natural units, $c=k_B=\hbar=1$. In addition, we consider only the case for $\mu=0$, although a general approach is straightforward. By introducing a reference temperature, T_0, we define $\theta=T/T_0$, $\bar{p}=p^0/T_0$, $\vec{v}=\vec{p}/|\vec{p}|$, and using $p^0=|\vec{p}|$, we rewrite the equilibrium distribution as

$$f_{{\rm eq},E}(t,\vec{x},\bar{p},\vec{v})=\frac{1}{e^{\bar{p}\gamma(1-\vec{v}\cdot\vec{u})/\theta}+1}, \tag{4}$$

where the subscript E stands for "exact." The distribution $f_{{\rm eq},E}$ is expanded using tensorial polynomials $P^{(n)}$, for the angular contribution, and $F^{(k)}$, for the radial dependence, such that

$$f_{{\rm eq},E}(t,\vec{x},p,\vec{v})=\frac{1}{e^{\bar{p}}+1}\sum_{n,k}^{\infty}a_{\underline{i}}^{(nk)}(t,\vec{x})P_{\underline{i}}^{(n)}(\vec{v})F^{(k)}(\bar{p}). \tag{5}$$

Here, the $(2+1)$-momentum vectors have been expressed in polar coordinates, $p^\mu=(\bar{p},\bar{p}\cos\phi,\bar{p}\sin\phi)$ with $\vec{v}=(\cos\phi,\sin\phi)$ being a unit vector that carries the angular dependence ϕ, and the index $\underline{i}$ denotes a family of indices $i_1,\ldots,i_n\in\{1,2\}$ whose total number equals the order n of the tensor for the angular dependence, i.e., $P_{\underline{i}}^{(n)}$ and $a_{\underline{i}}^{(nk)}$ are tensors of rank n. Such an ansatz has been used by Romatschke *et al.* [17] to expand the Maxwell-Jüttner distribution. Employing the Gram-Schmidt procedure, the radial polynomials $F^{(k)}$ are constructed satisfying the orthogonality relation

$$\int_0^\infty\frac{d\bar{p}}{4\pi}w(\bar{p})F^{(k)}(\bar{p})F^{(l)}(\bar{p})=\Gamma_F^{(k)}\delta_{kl}, \tag{6}$$

and the angular ones are constructed by satisfying

$$\int_0^{2\pi}\frac{d\phi}{2\pi}P_{\underline{i}}^{m}(\phi)P_{\underline{j}}^{n}(\phi)=\Gamma_{P,\underline{i}\underline{j}}^{(m)}\delta_{mn}. \tag{7}$$

The resulting polynomials and Γ constants up to second order are given in Appendix A. With these polynomials and taking into account Eq. (5), one can show that up to second order in n and k, we get

$$a_{\underline{i}}^{(nk)}=\frac{g^{(n)}}{\Gamma_F^{(k)}}T_0\int\frac{d\bar{p}}{4\pi}\frac{d\phi}{2\pi}f_{eq,E}P_{\underline{i}}^{(n)}F^{(k)}, \tag{8}$$

with $g^{(0)}=1$, $g^{(1)}=2$, and $g^{(2)}=4$. The explicit form of $a^{(nk)}$ is given in Appendix B. Using Eq. (5), the definitions of the polynomials, and their orthogonality relations it can be easily shown that the moments up to second order can be written in

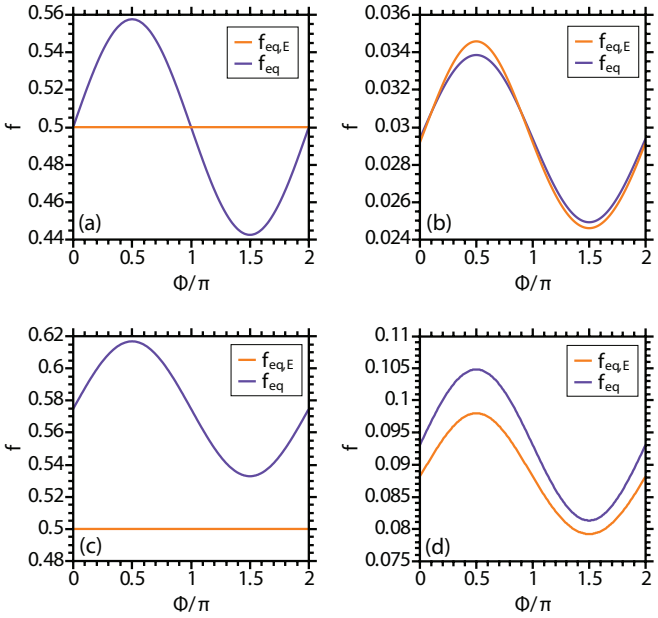

FIG. 1. (Color online) Comparison between the expanded Fermi dirac distribution $f_{\rm eq}$ and the full version $f_{{\rm eq},E}$ as a function of the angular component ϕ, for $\bar{p}=0$ (a and c) and $\bar{p}=3.5$ (b and d), with $\theta=1.0$ (a and b) and $\theta=1.5$ (c and d), $u^1=0.0$, $u^2=0.05$.

terms of the coefficients $a_{\underline{i}}^{(nk)}$ with $n,k\leqslant 2$ (see Appendix B), and therefore, the truncated expansion of the distribution $f_{\rm eq}$ up to second order becomes

$$f_{\rm eq}=\frac{1}{e^{\bar{p}}+1}\sum_{n=0}^{2}\sum_{k=0}^{2}a_{\underline{i}}^{(nk)}P_{\underline{i}}^{(n)}F^{(k)}. \tag{9}$$

This is sufficient to recover the moments

$$\langle p^{\alpha}\rangle_{\rm (eq)}=nU^{\alpha}, \tag{10a}$$

$$\langle p^{\alpha}p^{\beta}\rangle_{\rm (eq)}=(\epsilon+P)U^{\alpha}U^{\beta}-P\eta^{\alpha\beta}, \tag{10b}$$

of the full Fermi-Dirac distribution, Eq. (4). In Eq. (10b), we have introduced the Minkowski metric tensor $\eta^{\alpha\beta}$, the particle density $n=\frac{\pi}{48}T^2$, the pressure $P=\frac{9\zeta(3)}{\pi^2}nT$, and the energy density $\epsilon=2P$, where ζ denotes the Riemann ζ function, $\zeta(3)\approx 1.202$.

Figure 1 shows that the quality of the matching between the truncated $f_{\rm eq}$ and the exact $f_{{\rm eq},E}$, for $\bar{p}\sim 0$, is very poor, in contrast with the case $\bar{p}\sim 3.5$. However, this is not surprising, since we are dealing with a gas of ultrarelativistic particles which are always moving at the Fermi speed, and therefore none of them has energy $\bar{p}=0$. On the other hand, the matching is reasonable for $\theta=1$, while being off for $\theta>1$. Thus, we conclude that $\theta=1$ offers the best approximation, and therefore we work with that value. In addition, we have found that θ cannot be chosen far below unity because $f_{\rm eq}$ can present negative values. The fact that $\theta=1$ implies that the reference temperature T_0 should be equal to the temperature of the electronic gas T.

By making the expansion in polar coordinates, some questions naturally arise. While in the nonrelativistic case, where the Maxwell-Boltzmann distribution is expanded in Hermite polynomials, the projection coefficients are directly mapped to the moments of the distribution, in the relativistic case, the relation of the coefficients of the expansion with physical quantites is not straightforward. In our expansion, the coefficients due to the radial expansion [polynomials $F^{(k)}(\bar{p})$] can be mapped on the 0th component of the moments of the Fermi-Dirac distribution, while the angular expansion [polynomials $P_{\underline{i}}^{(k)}(\vec{v})$] coefficients contain the information on how these 0th components, normally containing limiting quantities like the Fermi speed or the total energy of the fluid, are distributed over the spatial components and directions of motion. Note that in the relativistic regime the components of the moments of the distribution are not independent like in the nonrelativistic case, e.g., for the first moment of the distribution we have $\langle p^0\rangle=\sqrt{n^2+\langle p^1\rangle^2+\langle p^2\rangle^2}$.

Another aspect that needs to be discussed is the convergence of the expansion. The expansion introduced here is valid if $\int f_{{\rm eq},E}^2/w(\bar{p})d\mu<\infty$ [31]. By manipulating this integral and studying the limiting cases, we arrive at the conclusion that the condition $2\gamma(1-|\vec{u}|)/\theta>1$ needs to be satisfied. By matching the Fermi-Dirac distribution we already found that $\theta=1$ offers the best fitting. Therefore, the convergence condition can be written as $2\sqrt{(1-|\vec{u}|)/(1+|\vec{u}|)}>1$, obtaining $|\vec{u}|<0.6v_F$. This relation is satisfied automatically since the hydrodynamic approach in graphene is valid only for small velocities ($|\vec{u}|\ll v_F$). Temperature variations around $\theta=1$ are also allowed as long as the convergence condition is satisfied and the expanded distribution remains positive.

B. Momentum space discretization

We now need to discretize the momentum space into a finite number N of discrete momentum vectors, p_q^{μ} (with $q=0,\ldots,N$), such that we can replace integrals in the continuum momentum space by sums over a small number of discrete momentum $(2+1)$-vectors. In order to do that, we use the Gaussian quadrature [32]. As an example, for the radial dependence of the expansion, in order to satisfy

$$\int_0^{\infty}\frac{d\bar{p}}{4\pi}w(\bar{p})F^{(k)}(\bar{p})\bar{p}^l=\sum_{q'=0}^{N}\frac{\omega_{q'}^{(\bar{p})}}{w(\bar{p}_{q'})}w(\bar{p}_{q'})F^{(k)}(\bar{p}_{q'})\bar{p}_{q'}^l, \tag{11}$$

for $k,l\leqslant 2$, we should calculate the discrete $\bar{p}_{q'}$ and respective radial weights $\omega_{q'}^{(\bar{p})}$. By using the Gaussian quadrature theorem, we found the following values:

$$\bar{p}_1=0.484,\quad \omega_1^{(\bar{p})}=0.0369,$$
$$\bar{p}_2=2.447,\quad \omega_2^{(\bar{p})}=0.0176,$$
$$\bar{p}_3=6.424,\quad \omega_3^{(\bar{p})}=0.000719.$$

Note that in fact, $\bar{p}$ is always larger than zero, as expected for ultrarelativistic particles (see Appendix C for numerical values with higher precision).

On the other hand, by following a similar procedure, we can calculate the N' discrete angles $\phi_{q''}$ and angular weights $\omega_{q''}^{(\phi)}$ (with $q''=1,\ldots,N'$), such that, for the angular integrals

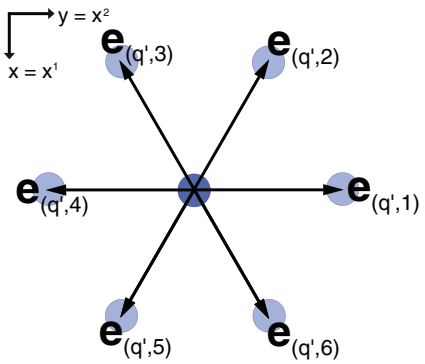

FIG. 2. (Color online) The populations $f_{\mathbf{q}}$ are moved between the nodes of a hexagonal lattice which are linked by the vector $\vec{e}_{\mathbf{q}}\delta t$.

over $P^{(n)}(v_i)^l(v_j)^m$, one gets

$$\int_0^{2\pi}\frac{d\phi}{2\pi}P^{(n)}(v_i)^l(v_j)^m=\sum_{q''=0}^{N'}\omega_{q''}^{(\phi)}P^{(n)}(v_{i,q''})^l(v_{j,q''})^m, \tag{12}$$

where $v_{i,q''}$ denotes $v_i(q'')$. The above expression is required to be an exact quadrature formula for $n\leqslant 2$ and $l+m\leqslant 2$. The results for the discrete angles and weight functions are $\phi_{q''}=\frac{\pi}{2}+(q''-1)\frac{\pi}{3}$ and $\omega_{q''}^{(\phi)}=\frac{1}{6}$ with $N'=6$.

By combining the radial and angular dependence of the discrete momentum $(2+1)$-vectors we get a total of 18 discrete lattice vectors $p_{\mathbf{q}}^{\mu}=p_{(q',q'')}^{\mu}=T_0(\bar{p}_{q'},\bar{p}_{q'}\cos\phi_{q''},\bar{p}_{q'}\sin\phi_{q''})$, where we have introduced the index $\mathbf{q}=(q',q'')$. This lattice cell configuration is shown in Fig. 2, where we can observe that, for recovering hydrodynamics in graphene, we need a hexagonal lattice. This is a very convenient result, since due to the fact that it possesses the same honeycomb lattice symmetries of graphene we can reproduce with good accuracy boundary conditions when modeling nanoribbons or other complex structures.

The exact quadrature relations, Eqs. (11) and (12), ensure that the moments up to second order are still represented exactly:

$$\langle p^{\alpha}\rangle_{(\mathrm{eq})}=\sum_{\mathbf{q}}\frac{\omega_{\mathbf{q}}}{w(\bar{p}_{\mathbf{q}})}f_{(\mathrm{eq}),\mathbf{q}}p_{\mathbf{q}}^{\alpha}, \tag{13a}$$

$$\langle p^{\alpha}p^{\beta}\rangle_{(\mathrm{eq})}=\sum_{\mathbf{q}}\frac{\omega_{\mathbf{q}}}{w(\bar{p}_{\mathbf{q}})}f_{(\mathrm{eq}),\mathbf{q}}p_{\mathbf{q}}^{\alpha}p_{\mathbf{q}}^{\beta}. \tag{13b}$$

We have expanded and discretized the Fermi-Dirac equilibrium distribution for ultrarelativistic particles. Note that the Grad-Schmidt procedure described here for the Fermi-Dirac distribution allows one to perform the expansion to higher orders without any problem, since the integrals in polar coordinates can be written with a recurrence formula for a given nth order. However, their analytical expressions become more difficult to manipulate due to the large number of terms. Now, we proceed to discretize the Boltzmann equation and find the evolution equation for the nonequilibrium distribution.

C. Lattice Boltzmann algorithm

With the expanded distribution functions and the discretization of momentum space at hand, we may use the following discrete Boltzmann equation [13,17,21],

$$f_{\mathbf{q}}(t+\delta t,\vec{x}+\vec{e}_{\mathbf{q}}\delta t)-f_{\mathbf{q}}(t,\vec{x})=-\frac{p^{\alpha}U_{\alpha}}{p^0\tau}[f_{\mathbf{q}}(t,\vec{x})-f_{\mathrm{eq},\mathbf{q}}(t,\vec{x})], \tag{14}$$

where we have introduced the notations $\vec{e}_{\mathbf{q}}=\vec{p}_{\mathbf{q}}/p^0$ and $f_{\mathbf{q}}(t,\vec{x})=f(t,\vec{x},p_{\mathbf{q}})$. Note that $\vec{e}_{\mathbf{q}}$ are unit vectors, which means that there are effectively six different $\vec{e}_{\mathbf{q}}$. The discrete Boltzmann equation is now embedded into a lattice, and each time step of $\delta t=1$ corresponds to one execution of the following steps:

(1) Calculate the equilibrium distributions $f_{\mathrm{eq},\mathbf{q}}(t,\vec{x})$ from Eq. (9) using the macroscopic variables $n=n(t,\vec{x})$, $\vec{u}=\vec{u}(t,\vec{x})$, and $T(t,\vec{x})$. At $t=0$, $n(t=0,\vec{x})$, $T(t=0,\vec{x})$, and $\vec{u}(t=0,\vec{x})$ are imposed as initial conditions.

(2) Collision: Introducing the postcollisional distributions $f'_{\mathbf{q}}$, calculate

$$f'_{\mathbf{q}}(t,\vec{x})=f_{\mathbf{q}}(t,\vec{x})-\frac{p^{\alpha}U_{\alpha}}{p^0\tau}[f_{\mathbf{q}}(t,\vec{x})-f_{\mathrm{eq},\mathbf{q}}(t,\vec{x})].$$

At $t=0$, take $f_{\mathbf{q}}=f_{\mathrm{eq},\mathbf{q}}$.

(3) Streaming: Move the $f'_{\mathbf{q}}$ along $\vec{e}_{\mathbf{q}}$:

$$f_{\mathbf{q}}(t+1,\vec{x}+\vec{e}_{\mathbf{q}})=f'_{\mathbf{q}}(t,\vec{x}).$$

(4) Calculate the new macroscopic variables. First we compute the energy density of the system by solving the eigenvalue problem, $\langle p^{\alpha}p^{\beta}\rangle U_{\alpha}=\epsilon U^{\beta}$, according to the Landau-Lifshitz decomposition [18]. From this, we get ϵ and U^{α}. Next, we use the relation $n=\langle p^{\alpha}\rangle U_{\alpha}=n$ to obtain the particle density. Here, the average values, $\langle p^{\alpha}\rangle$ and $\langle p^{\alpha}p^{\beta}\rangle$, are simply

$$\langle p^{\alpha}\rangle=\sum_{\mathbf{q}}\frac{\omega_{\mathbf{q}}}{w(\bar{p}_{\mathbf{q}})}f_{\mathbf{q}}p_{\mathbf{q}}^{\alpha},$$

$$\langle p^{\alpha}p^{\beta}\rangle=\sum_{\mathbf{q}}\frac{\omega_{\mathbf{q}}}{w(\bar{p}_{\mathbf{q}})}f_{\mathbf{q}}p_{\mathbf{q}}^{\alpha}p_{\mathbf{q}}^{\beta}.$$

The streaming step indicates that if we discretize the real space based on a hexagonal lattice where the sites are linked by $\vec{e}_{\mathbf{q}}\delta t$, as shown in Fig. 2, the values of $f_{\mathbf{q}}$ will be moved between these sites exactly. This is known as "exact streaming" and is crucial for the computational efficiency and accuracy of the lattice Boltzmann methods.

In summary, we have developed a $(2+1)$-dimensional relativistic lattice Boltzmann scheme with the remarkable feature that it takes into account the Fermi-Dirac statistics, while recovering all the moments up to second order. The discretization is realized on a hexagonal lattice such that exact streaming is achieved. The fact that the quadrature corresponds to a hexagonal lattice allows one to represent complex boundaries more precisely in graphene applications. This will be studied in more detail in future works.

Up to now, we have been working with undoped graphene, $\mu=0$. However, by using the same orthogonal polynomials, we can easily integrate the Fermi-Dirac statistics for the doped case, obtaining the extended formulation. In this work, we use $\mu=0$, in order to compare the results with previous models

in the literature that use the Maxwell-Jüttner distribution, since transport theory shows that, in the case of undoped Fermi-Dirac statistics, the transport coefficients, namely shear viscosity and thermal conductivity, have the same expressions as for the Boltzmann statistics [18]. Therefore, the shear viscosity takes the value of $\eta = (3/5)P(\tau - \delta t/2)$ [33]. Later, we use the doped case to study the Riemann problem, which to best of our knowledge has never been studied before. However, it is present when, for instance, laser beams are pointed to the graphene sheet in order to measure transport coefficients [34].

III. VALIDATION: RIEMANN PROBLEM

In order to validate our model, we solve the Riemann problem for the ultrarelativistic Fermi-Dirac gas. The Riemann problem is a standard test for both relativistic and nonrelativistic hydrodynamic numerical schemes, because it involves the evolution of two states of the fluid initially separated by a discontinuity. In our case, we set up an effectively one-dimensional system of $L_x \times L_y = 3000 \times 2$ nodes, using periodic boundary conditions in x and y components. Initially, there are two regions with particle densities, $n_0 = 1$ ($3L_x/4 > x > L_x/4$) and $n_1 = 0.41$ ($x \leqslant L_x/4$ and $x \geqslant 3L_x/4$), creating a rectangular plateau of nonzero particle density in the center of the simulation zone. Here we consider an initial constant temperature, $T_0 = 1$. The initial velocity is set to zero and the value of the relaxation time τ is calculated for two different values of $\xi = \eta/(P_0\delta t)$, with $P_0 = \frac{9\zeta(3)}{\pi^2} n_0 T_0$. The evolution of the system is displayed in Fig. 3 after 470 time steps, showing the generated shock wave. We have only plotted the region $x > L_x/2$ since the other one does not give additional information. Note that there is excellent agreement with the solutions provided by the model proposed in Ref. [26] for the same initial conditions.

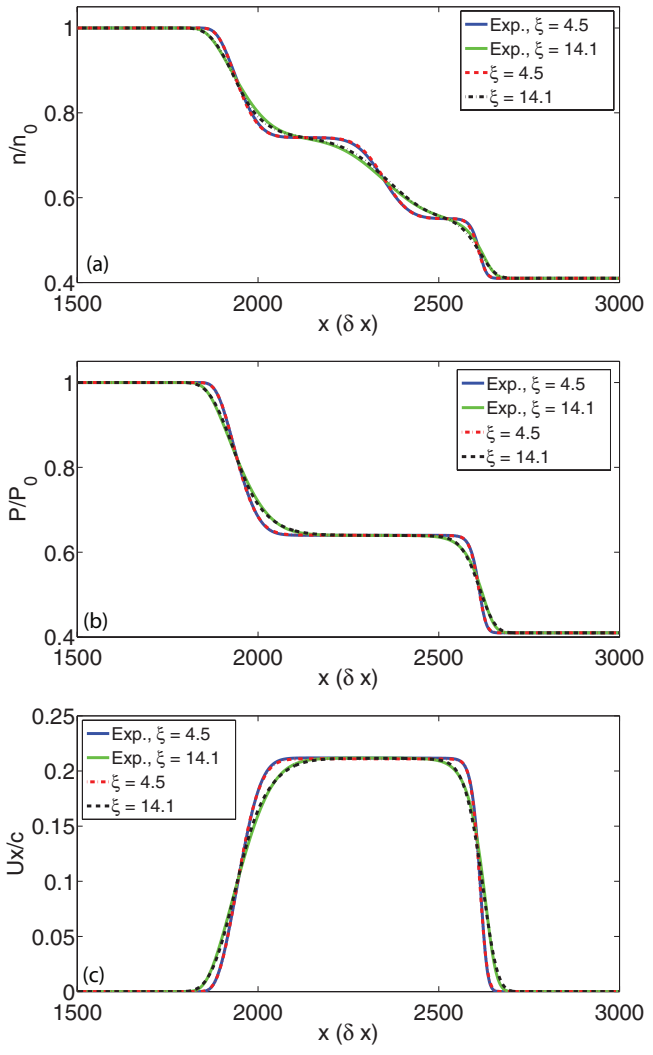

FIG. 3. (Color online) Density (a), pressure (b), and velocity (c) profiles for the solution of the Riemann problem. Here $\xi = \eta/(P_0\delta t)$ is a dimensionless number. The expected results were calculated using the model in Ref. [26].

IV. RIEMANN PROBLEM WITH $\mu \neq 0$

Let us now consider the case when the chemical potential μ is different from zero. For this purpose, we follow the same

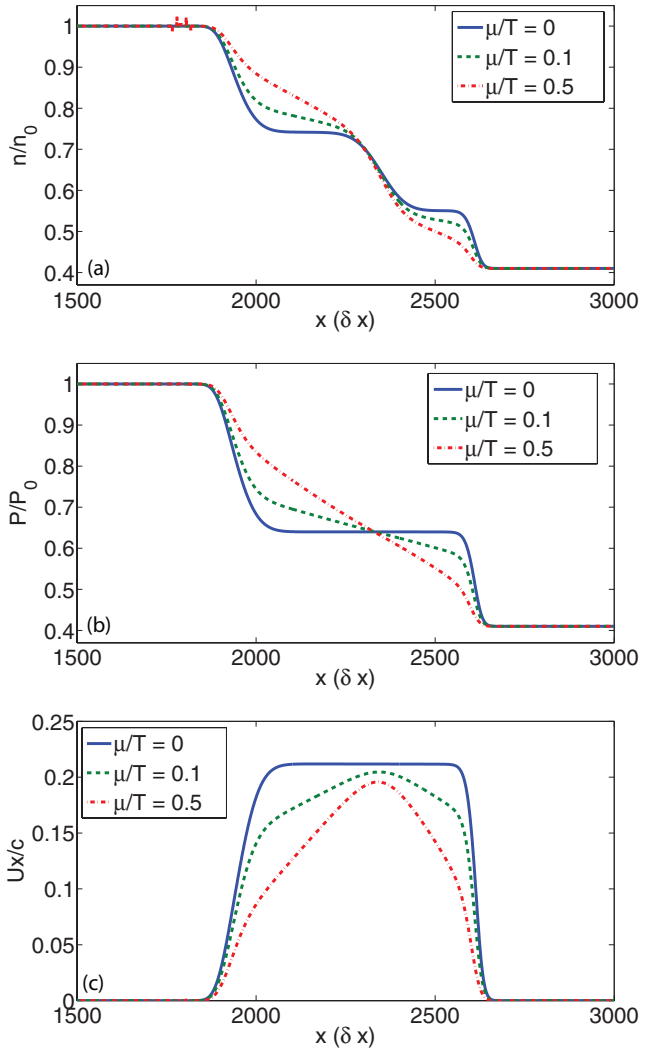

FIG. 4. (Color online) Density (a), pressure (b), and velocity (c) profiles of the solution of the Riemann problem, for different values of the chemical potential μ.

procedure described before but this time we keep $\mu \neq 0$. The development is straightforward, and therefore does not deserve a full explanation. The polynomials are the same as described in Appendix A, and the coefficients $a_{\underline{i}}^{(nk)}$ are calculated by using Eq. (8).

The hydrodynamic approach of electrons in graphene works for low doping, $\mu/k_BT \ll 1$ [7–9]. Therefore, we can expand the discrete equilibrium distribution in powers of μ/k_BT up to third order, neglecting errors of the order of $(\mu/k_BT)^4$. We perform additional simulations of the Riemann problem with the same parameters as before, but now varying the chemical potential. As we can observe from Fig. 4, increasing the chemical potential tends to increase also the effective viscosity of the system, smoothing the profiles of the velocity, pressure, and density. This result is very interesting because it suggests that, in fact, impurities with soft potentials (small μ/k_BT) in graphene samples can be treated as local modifications in the effective viscosity of the electronic fluid. In other words, this result suggests a promising way to include impurities in the hydrodynamic approach of electrons in graphene. Note that in this figure there is a noise in the profile of the particle density. This numerical instability remains with the same amplitude and is always located at the boundary when $n = n_0$, and therefore, it does not destroy the stability of the simulation. It can be due to the relevance of higher-order terms which are not recovered by our expansion.

V. CONCLUSIONS

We have derived a new family of orthogonal polynomials using as the weight function the Fermi-Dirac distribution for ultrarelativistic particles in two dimensions. By applying the Gaussian quadrature we have calculated the set of representative momentum $(2+1)$-vectors, which allows us to replace the integrals over the continuum momentum space by sums over such vectors. As a very interesting result, we have found that those vectors possess the same symmetries as the honeycomb lattice of carbon atoms in graphene, making possible the accurate implementation of complex boundary conditions in future applications, such as point defects and nanoribbons. The derivation has been performed by imposing that the expanded distribution should fulfill at least the first three moments of the equilibrium distribution, which are needed to recover the appropriate hydrodynamics. However, higher-order moments can also be recovered by using the same procedure in this paper.

In addition, we have developed a new lattice kinetic scheme to study the dynamics of the electronic flow in graphene. The model is validated on the Riemann problem, which is one of the most challenging tests in numerical hydrodynamics, presenting excellent agreement with previous models in the literature. By increasing the chemical potential, we have found that the profiles of the velocity, the particle density, and the pressure change similar to the case when the viscosity is increased, and we conclude that increasing the Fermi energy results in increasing the effective viscosity of the electronic fluid. This result suggests that soft impurities in graphene samples can be treated as local modifications of the viscosity; however, further studies must be performed in order to confirm this statement.

The fact that we can propagate the information from one site to another in an exact way, avoiding interpolation, removes any kind of round-off errors during the streaming. This property also implies a negative momentum diffusivity, $\propto P\delta t/2$, also known as propagation viscosity [35], which needs to be added to the collisional viscosity $(3/5)P\tau$ to form the effective viscosity of the fluid. We expect this model to be appropriated to study many problems in electronic transport in graphene in the framework of the hydrodynamic approach, e.g., turbulence and hydrodynamical instabilities in graphene flow, just to name a few.

Extensions of the present model to take into account higher-order moments of the Fermi-Dirac equilibrium distribution as well as the inclusion of the distribution and dynamics of holes will be a subject of future research.

ACKNOWLEDGMENTS

We acknowledge financial support from the European Research Council (ERC), Advanced Grant No. 319968-FlowCCS.

APPENDIX A: POLYNOMIALS AND Γ CONSTANTS

In this section, we write explicitly the family of polynomials, which are orthogonal using as the weighting function the Fermi-Dirac distribution at rest, with their respective normalization factors. For the case of the angular dependence, we have

$$\begin{aligned} P^{(0)}(\vec{v}) &= 1, \\ P_i^{(1)}(\vec{v}) &= v_i, \\ P_{ij}^{(2)}(\vec{v}) &= v_i v_j - \tfrac{1}{2}\delta_{ij}, \end{aligned}$$

with the following normalization factors:

$$\begin{aligned} \Gamma_P^{(0)} &= 1, \\ \Gamma_{P,ij}^{(1)} &= \tfrac{1}{2}\delta_{ij}, \\ \Gamma_{P,ijkl}^{(2)} &= \tfrac{1}{8}(\delta_{il}\delta_{jk} + \delta_{ik}\delta_{jl} - \delta_{ij}\delta_{kl}). \end{aligned}$$

For the case of the radial dependence, we have the polynomials

$$\begin{aligned} F^{(0)}(\bar{p}) &= 1, \\ F^{(1)}(\bar{p}) &= \bar{p} - c_{10}, \\ c_{10} &= \frac{\pi^2}{12\log(2)}, \\ F^{(2)}(\bar{p}) &= \bar{p}^2 - c_{21}\bar{p} - c_{20}, \\ c_{21} &= -\frac{6[7\pi^4\log(2) - 15\pi^2\zeta(3)]}{5[\pi^4 - 216\log(2)\zeta(3)]}, \\ c_{20} &= \frac{7\pi^6 - 3240\zeta(3)^2}{10[\pi^4 - 216\log(2)\zeta(3)]}, \end{aligned}$$

with ζ denoting the Riemann ζ function. The normalization factors for these polynomials are

$$\Gamma_F^{(0)} = \frac{\log(2)}{4\pi}, \quad \Gamma_F^{(1)} = -\frac{\pi^3}{576\log(2)} + \frac{3\zeta(3)}{8\pi},$$
$$\Gamma_F^{(2)} = \frac{1}{400\pi}\left(\frac{49\pi^8\log(2) - 210\pi^6\zeta(3) + 48\,600\zeta(3)^3}{\pi^4 - 216\log(2)\,\zeta(3)} + 2250\zeta(5)\right).$$

APPENDIX B: COEFFICIENTS FOR THE EXPANSION OF $f_{\rm eq}$ AND RELATION TO MOMENTS

The coefficients of the expansion in Eq. (9) are given by

$$a^{(00)} = \theta, \quad a_i^{(10)} = 2\,\theta\frac{1}{\gamma+1}u_i\gamma,$$
$$a_{ij}^{(20)} = \sigma_{ij}\,4\,\theta\frac{1}{(\gamma+1)^2}\left[\gamma^2\left(u_iu_j - \frac{1}{2}\delta_{ij}\right)\gamma^2 + \frac{1}{2}\delta_{ij}\right],$$
$$a^{(01)} = \alpha^{(1)}\theta\,[\theta\gamma - 1]\,,$$
$$a_i^{(11)} = \frac{2\alpha^{(1)}\theta}{\gamma+1}\,[\theta(\gamma+1) - 1]\,u_i\gamma,$$
$$a_{ij}^{(21)} = \frac{4\alpha^{(1)}\theta}{(\gamma+1)^2}[(2-\delta_{ij})\theta(\gamma+2) - \sigma_{ij}] \times [\gamma^4(u_iu_j - \delta_{ij}/2) + \delta_{ij}/2],$$
$$a^{(02)} = \alpha^{(2)}\theta\{\beta^{(2|1)}(\theta\gamma - 1) + \beta^{(2|2)}[(3\theta\gamma - 2) - \theta] + \beta^{(2|3)}[\theta^2(3\gamma^2 - 1) - 2]\},$$
$$a_i^{(12)} = \frac{2\alpha^{(2)}\theta}{\gamma+1}\{\beta^{(2|1)}[\theta(\gamma+1) - 1] + \beta^{(2|2)}\theta(3\theta\gamma - 2)(\gamma+1) + \beta^{(2|3)}[3\theta^2\gamma(\gamma+1) - 2]\}u_i\gamma,$$
$$a_{ij}^{(22)} = \frac{4\alpha^{(2)}\theta}{(\gamma+1)^2}\{\beta^{(2|1)}[(2-\delta_{ij})\theta(\gamma+2) - (2\delta_{ij}+1)\sigma_{ij}] + \beta^{(2|2)}3\theta^2(\gamma+1)^2 - 2(2-\delta_{ij})[\theta(\gamma+2) - 2\delta_{ij}\sigma_{ij})] + \beta^{(2|3)}[3\theta^2(\gamma+1)^2 - 2\sigma_{ij}]\}\left[\gamma^2\left(u_iu_j - \frac{1}{2}\delta_{ij}\right)\gamma^2 + \tfrac{1}{2}\delta_{ij}\right],$$

where $\sigma_{ij} = (-1)^{\delta_{2,i}\delta_{2,j}}$ or

$$(\sigma_{ij}) = \begin{pmatrix} 1 & 1 \\ 1 & -1 \end{pmatrix}, \tag{B1}$$

and

$$\alpha^{(1)} = \frac{12\pi^2\log(2)}{216\log(2)\zeta(3) - \pi^4},$$
$$\alpha^{(2)} = 5\{2250\zeta(5)[216\log(2)\zeta(3) - \pi^4] + 210\pi^6\zeta(3) - 49\pi^8\log(2) - 48\,600\zeta(3)^3\}^{-1},$$
$$\beta^{(2|1)} = -14\pi^6\log(2),$$
$$\beta^{(2|2)} = -15\pi^4\zeta(3)^2,$$
$$\beta^{(2|3)} = 3240\log(2)\zeta(3)^2,$$

which are approximately $\alpha^{(1)} \approx 0.994$, $\alpha^{(2)}\beta^{(2|1)} \approx -1.629$, $\alpha^{(2)}\beta^{(2|2)} \approx -0.307$, and $\alpha^{(2)}\beta^{(2|1)} \approx 0.567$.

To obtain the moments from the expansion of $f_{\rm eq}$, we expressed them in terms of the $a_{\underline{i}}^{(nk)}$ using Eqs. (8) and (9) and the expressions in Appendix A, e.g., $\langle p^0\rangle = T_0^2(\Gamma_F^{(1)}a^{(01)} + c_{10}\Gamma_F^{(0)}a^{(00)})$.

Note that for the calculation of the coefficients $a_{\underline{i}}^{(nk)}$ we should use the integration formula

$$\int_0^\infty dx\,\frac{x^{n-1}}{z^{-1}e^{a\,x} + 1} = -z^{-1}a^{-n}\Gamma(n)\,\mathrm{Li}_n(-z),$$

which holds for $n > 0$, $a \in \mathbb{R}$, and $a > 0$. Here, $\Gamma(n)$ denotes the Γ function, which becomes $\Gamma(n) = (n-1)!$ for $n \in \mathbb{N}$. $\mathrm{Li}_n(z)$ is the polylogarithm which can be defined using a power series: $\mathrm{Li}_n(z) = \sum_{k=1}^\infty \frac{z^k}{k^n}$. If we consider the chemical potential in the Fermi-Dirac distribution to be zero, we have $z = 1$ and the relevant values of the polylogarithm become $\mathrm{Li}_1(-1) = -\log(2)$, $\mathrm{Li}_2(-1) = -\frac{\pi^2}{12}$, and $\mathrm{Li}_3(-1) = -\frac{3}{4}\zeta(3)$. On the other hand, for $\mu \neq 0$, we take $z = e^{\mu/T}$.

APPENDIX C: RESULTS FOR RADIAL GAUSSIAN QUADRATURE

When the radial Gaussian quadrature is applied, the following values for the discrete $\bar{p}_i$ are obtained:

$$\bar{p}_1 = 0.484\,053\,475\,155\,406\,063\,755\,079\,436\,159\,1,$$
$$\bar{p}_2 = 2.446\,744\,868\,967\,085\,266\,875\,118\,980\,420\,0,$$
$$\bar{p}_3 = 6.424\,352\,261\,225\,515\,256\,585\,901\,256\,325\,4,$$

with its respective weight functions

$$\omega_1^{(\bar{p})} = 0.036\,873\,061\,135\,963\,836\,010\,154\,242\,597\,8,$$
$$\omega_2^{(\bar{p})} = 0.017\,566\,680\,177\,745\,899\,345\,375\,761\,739\,0,$$
$$\omega_3^{(\bar{p})} = 0.000\,719\,158\,724\,453\,162\,993\,584\,103\,692\,7.$$

[1] K. Novoselov, A. Geim, S. Morozov, D. Jiang, M. Katsnelson, I. Grigorieva, and S. Dubonos, Nat. Lett. **438**, 197 (2005).

[2] K. S. Novoselov, A. K. Geim, S. V. Morozov, D. Jiang, Y. Zhang, S. V. Dubonos, I. V. Grigorieva, and A. A. Firsov, Science **306**, 666 (2004).

[3] D. P. DiVincenzo and E. J. Mele, Phys. Rev. B **29**, 1685 (1984).

[4] S. Das Sarma, S. Adam, E. H. Hwang, and E. Rossi, Rev. Mod. Phys. **83**, 407 (2011).

[5] A. K. Geim and A. H. MacDonald, Phys. Today **60**, 35 (2007).

[6] M. Müller, J. Schmalian, and L. Fritz, Phys. Rev. Lett. **103**, 025301 (2009).

[7] M. Müller and S. Sachdev, Phys. Rev. B **78**, 115419 (2008).

[8] L. Fritz, J. Schmalian, M. Müller, and S. Sachdev, Phys. Rev. B **78**, 085416 (2008).
[9] M. Müller, L. Fritz, and S. Sachdev, Phys. Rev. B **78**, 115406 (2008).
[10] M. Mendoza, H. J. Herrmann, and S. Succi, Phys. Rev. Lett. **106**, 156601 (2011).
[11] M. Mendoza, H. J. Herrmann, and S. Succi, Sci. Rep. **3**, 1052 (2013).
[12] M. Mendoza, B. M. Boghosian, H. J. Herrmann, and S. Succi, Phys. Rev. Lett. **105**, 014502 (2010).
[13] M. Mendoza, B. M. Boghosian, H. J. Herrmann, and S. Succi, Phys. Rev. D **82**, 105008 (2010).
[14] D. Hupp, M. Mendoza, I. Bouras, S. Succi, and H. J. Herrmann, Phys. Rev. D **84**, 125015 (2011).
[15] Z. Xu and C. Greiner, Phys. Rev. C **71**, 064901 (2005).
[16] I. Bouras, E. Molnar, H. Niemi, Z. Xu, A. El, O. Fochler, C. Greiner, and D. H. Rischke, Phys. Rev. Lett. **103**, 032301 (2009).
[17] P. Romatschke, M. Mendoza, and S. Succi, Phys. Rev. C **84**, 034903 (2011).
[18] C. Cercignani and G. M. Kremer, *The Relativistic Boltzmann Equation: Theory and Applications* (Birkhauser, Boston, Basel, Berlin, 2002).
[19] X. He and L.-S. Luo, Phys. Rev. E **56**, 6811 (1997).
[20] N. S. Martys, X. Shan, and H. Chen, Phys. Rev. E **58**, 6855 (1998).
[21] X. He and L.-S. Luo, Phys. Rev. E **55**, R6333 (1997).
[22] S. Succi, *The Lattice Boltzmann Equation for Fluid Dynamics and Beyond* (Clarendon Press and Oxford University Press, Oxford and New York, 2001).
[23] T. Abe, J. Comp. Phys. **131**, 241 (1997).
[24] X. Shan and X. He, Phys. Rev. Lett. **80**, 65 (1998).
[25] X. Shan, X.-F. Yuan, and H. Chen, J. Fluid Mech. **550**, 413 (2006).
[26] M. Mendoza, I. Karlin, S. Succi, and H. J. Herrmann, Phys. Rev. D **87**, 065027 (2013).
[27] M. Y. Han, B. Özyilmaz, Y. Zhang, and P. Kim, Phys. Rev. Lett. **98**, 206805 (2007).
[28] V. Barone, O. Hod, and G. E. Scuseria, Nano Lett. **6**, 2748 (2006).
[29] F. Jüttner, Z. Phys. **47**, 542 (1928).
[30] M. Mendoza, N. A. M. Araújo, S. Succi, and H. J. Herrmann, Sci. Rep. **2**, 611 (2012).
[31] H. Grad, Commun. Pure Appl. Math. **2**, 331 (1949).
[32] P. J. Davis and P. Rabinowitz, *Methods of Numerical Integration*, 2nd ed. (Academic Press, Orlando, 1984).
[33] M. Mendoza, I. Karlin, S. Succi, and H. J. Herrmann, J. Stat. Mech. (2013) P02036.
[34] J.-U. Lee, D. Yoon, H. Kim, S. W. Lee, and H. Cheong, Phys. Rev. B **83**, 081419 (2011).
[35] S. Ubertini, G. Bella, and S. Succi, Phys. Rev. E **68**, 016701 (2003).